MEASURING 3D DEFORMATIONS IN THE PROCESS OF WELDING

Mjerenje 3D deformacija u procesu zavarivanja

Ján Urminský[1], Milan Marônek[1], Jozef Bárta[1]

[1]Slovak University of Technology in Bratislava, Faculty of Materials Science and Technology in Trnava, Institute of Production Technologies, J. Bottu 25, 917 24 Trnava

Ključne riječi: *Zavarivanje, mjerenje deformacija u realnom vremenu, GOM ARAMIS, GOM ATOS*

Sažetak

Rad se bavi mjerenjem deformacija zavarenih spojeva pomoću optičkog 3D skanera. Zglobovi zavarenih spojeva proizvedeni su pomoću potrošne elektrode u inertnom plinu (131). Za eksperimentalno mjerenje deformacija zavarivanja korišteno je GOM ATOS II TripleScan SO MV320 uređaj kapaciteta 320 × 240 × 240 mm i razlučivost kamere od 5,0 MPx. Softverski modul GOM ARAMIS Pro korišten je za određivanje tijeka deformacija zavarivanja u stvarnom vremenu u stvarnom vremenu. Analiza podataka ukazuje na to da veća količina ukupne topline koja se isporučuje u zavarivanje nastoji proizvesti veće kutne deformacije i odstupanja oblika.

Key words: *Welding, measurement of deformations in real time, GOM ARAMIS, GOM ATOS*

Abstract

The paper deals with measuring the weld joint deformations using an optical 3D scanner. The fillet weld joints were fabricated by the consumable electrode in inert gas (131). The GOM ATOS II TripleScan SO MV320 device with a measuring capacity of 320 × 240 × 240 mm and a camera resolution of 5.0 MPx was used for experimental measurement of the weldment deformations. The GOM ARAMIS Pro software module was used to determine the course of real-time weldment deformations in real time. The data analysis indicates that higher amount of the total heat supplied into the weldment tends to produce larger angular deformations and shape deviations.

1. Introduction

Weldment deformations represent a frequent accompanying phenomenon in the weld joints fabrication. It is particularly due to financial reasons that the current methods of measuring the deformations of weld joints generally use simple instruments and devices. In the case of free-form structures and when a many repetitions are required, the analyses are quite time consuming. Human factor has a significant influence on the measurement accuracy. Besides architecture and reverse engineering, modern 3D scanning methods are finding increasing application in the field of engineering production technology [1]. In addition to optical scanning that provides the resulting digital model of the object measured, optical 3D scanners can measure and determine the course of deformations (point displacement) under load at a specified scanning frequency. All individual optical 3D scanners are just the devices capable of capturing an image or recording a video. The scanned image must be processed prior to measurement. The image processing requires the computer software capable of working with and analysing the image data. It is essentially a matter of the scientific fields dealing with the computer and machine vision and image processing. The idea of developing a computer vision has been explored by experts in the 1960s. Forty years later, the issue still remained uninvestigated. The object geometry described by lines, curves, and angles is known as Euclidean geometry.

Yet, in case of computer vision and image processing, the Euclidean geometry is not precise enough. In computer vision, perspective space serves as a convenient way to represent objects in the 3D world, and can be expanded to the three dimensional projection spaces [2]. When processing digital images, reference surface points must be determined. Software then uses orientation and displacement of the reference points to calculate deformations and stresses in the object being measured. The processed image is then transformed into the black-and-white one with grayscale transition in 256 levels. The reference points are determined based on the contrast between the black and white colours of the pattern applied to the object being measured.

The software can identify the position of the reference points based on the grey colour value from the gradient of transition from black to white. The system is used to measure real-time deformations and strains. Fragments of each scanned image are defined. The fragments consist of a certain number of pixels forming the image. The fragment centre represents an identification point. Identification of the areas in several consecutive images is called matching. Digital Image Correlation (DIC) logarithms for images correlation or the method of smallest squares are used for the Fractional Fragmentation Evaluation. The key assumption is that there is a correlation between the original and the deformed state of the fragment. The correlation function determines the similarity rate of the two fragments.

$$\boldsymbol{f}(\boldsymbol{x},\boldsymbol{y}) \overset{!}{\leftrightarrow} \boldsymbol{g}(\boldsymbol{x_t},\boldsymbol{y_t}) \tag{1}$$

Scalar product can be used to determine the deviations in the respective direction.

$$\boldsymbol{c}(\Delta\boldsymbol{x},\Delta\boldsymbol{y}) = \frac{\langle \boldsymbol{f}(\boldsymbol{x},\boldsymbol{y}), \boldsymbol{g}(\boldsymbol{x}+\Delta\boldsymbol{x},\boldsymbol{y}+\Delta\boldsymbol{y})\rangle}{|\boldsymbol{f}(\boldsymbol{x},\boldsymbol{y})| \cdot |\boldsymbol{g}(\boldsymbol{x},\boldsymbol{y})|} \tag{2}$$

The software algorithm allows for the similarity determination of two images based on its ability to discriminate various locations of various changes of the fragment structure shape. Image interpolation is used to determine the similarity of images. Based on iterative (chain) algorithms, transition areas with a high number of grey levels are minimised [3, 4, 5].

2. Experimental methods

The Al 5083-H111 aluminium alloy was selected for experimental measurements. Its chemical composition is shown in Table 1. Similarly to other 5000 alloy series, it is reinforced by a solid magnesium solution in an aluminium matrix. It achieves elevated strength values that are rather due to cold-rolling deformation ("H" state) than to heat treatment. The Al 5083 alloy achieves the highest strength of all alloys in the H state (275-350 MPa) [6, 7, 8, 9].

It is famous for its excellent applicability under extreme conditions. It is highly resistant to the effects of seawater and industrial chemicals. Since the alloy can withstand extremely low temperatures, it is particularly suited for the structures operating under cryogenic conditions. Its low specific gravity and high corrosion resistance make it predestined for fatigue-loaded components of ships, railway wagons, as well as parts of passenger cars, lorries and pressure vessels. Alloys with more than 3.5% Mg content are prone to corrosion cracking, which limits its use up to 65° C. Compared to other aluminium alloys, it exhibits good weldability with all the available arc and resistance welding technologies. It is particularly suitable for MAG and TIG welding technologies widely used in fabrication of weld joints. Welding under the deformation stiffness conditions reduces the strength of heat-affected zone [2, 10, 11, 12, 13].

Table 1 Chemical composition of the Al5083-H111 Al compound

Chemical element	Al	Mg	Si	Cr	Mn	Cu
Chem. composition [wt. %]	94.10	4.72	0.43	0.20	0.30	0.25

The fillet joints in two different configurations (Figure 1) of 50 x 200 mm metal sheets by a thickness of 2 mm were prepared for the experiment. The weld joints were made by 131 method; the welding position was horizontal vertical (PB). The Fronius TPS600i welding device was used as welding machine. The device disposes the systems enabling precise control of the required welding parameters. Welding was performed at the Workplace of the arc and plasma technologies, Institute of Production Technologies, STU Faculty of Materials and Technology in Trnava. It is an automated welding workplace where the welding process can be performed using a programmable portal device. The welding process is fully programmable with the back-check option.

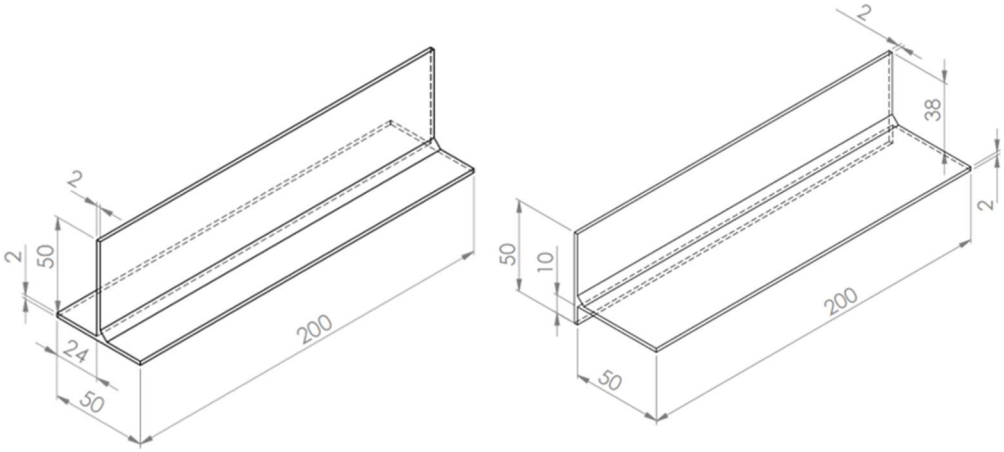

Fig. 1 Geometry of weldments; variant A, variant B

The GOM ATOS II TripleScan scanner with a resolution of 5 MPix and a measurement volume of the MV320, 320×240×240 mm was used for scanning. The GOM ARAMIS Professional 2016 software was used to prepare the measurement records. The software is able to communicate with the GOM Co. devices that are primarily used for optical 3D scanning and component digitisation. The type of weld joint and the associated welding position of weldments was designed so that to avoid illuminating the scanner cameras by the light source occurring during the welding process, and also to avoid extensive heat removal from the weldments. Prior to scanning, a stochastic pattern had to be applied to the weld area to be monitored. The structured pattern was made using the paint resistant to the heat up to 800° C, which was selected with respect to the melting temperature of the Al5083-H111 base material used (638 °C).

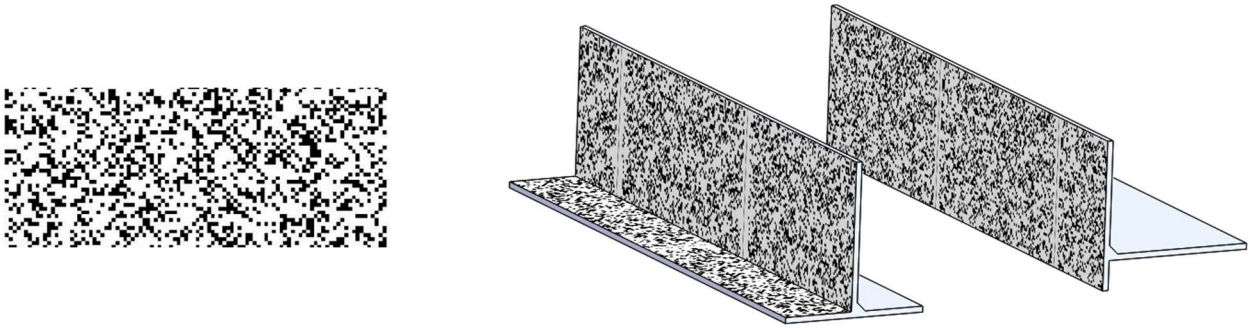

Fig. 2 Structured random pattern, the pattern placement in the monitored weldments surface

After applying the structured pattern to the weldment area, colour curing at the temperature of 250 ° C for 1 hour followed. After such sample preparation, experimental measurements were performed.

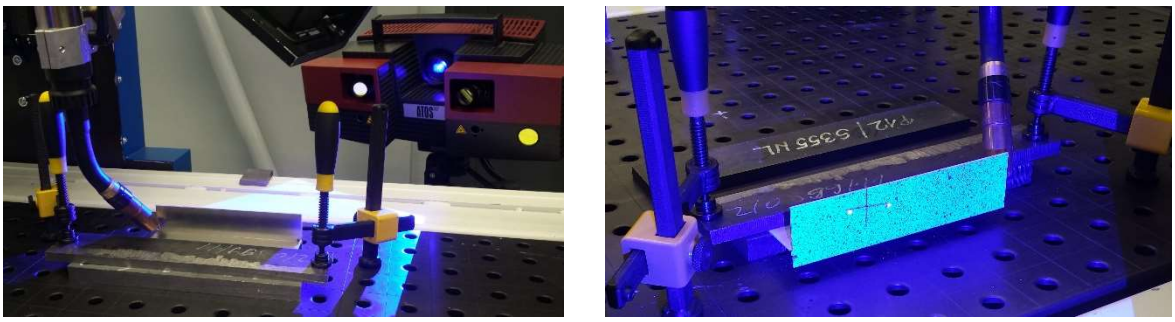

Fig. 3 Experimental measurement of the weldment joints deformations by the GOM ATOS II TripleScan scanner

The welding parameters of the Al5083-H111 Al alloy are shown in Tables No. 2 and 3. Welding current and wire feed rate varied based on the welding parameters. The filler material of AlSi5 with a diameter of 1.2 mm was used for welding. AlSi5 is the most commonly used filler wire for welding aluminium alloys. The silicon content reduces the melting temperature, and the weld joint is not prone to cracking. Pure argon (Ar 100%) was used as shielding gas. The flow rate of shielding gas was set at 15 l/min.

Table 2 Parameters of welding, A variant

Specimen No.	*I [A]*	*U [V]*	v_z *[mm/s]*	v_p *[mm/s]*
1A	80	18.0	15	5.2
2A	90	18.5	15	5.3
3A	100	18.8	15	5.4

Table 3 Parameters of welding, B variant

Specimen No.	*I [A]*	*U [V]*	v_z *[mm/s]*	v_p *[mm/s]*
1B	80	18.0	15	5.2
2B	90	18.5	15	5.3
3B	100	18.8	15	5.4

Real-time measurement of the weldments deformation course was performed at 15 Hz using the GOM ATOS II TripleScan equipment and GOM ARAMIS program module. After a certain cooling time, a time record of the welding process was elaborated. The record can be then digitally processed and analysed. The GOM Correlate 2016 analytical software is able to determine the values of angular deformations and shape changes of both weldments and stresses generated during welding.

3. Experiment evaluation

The course of angular deformation of weldments depends on the weld geometry, welding parameters and the heat supplied to the weldment. The welding time (*tz*) and the welding length (*Lz*) were determined from the data obtained by the GOM ATOS II TripleScan optical 3D scanner. The measured thermal input was calculated according to the formula No. 3.

$$Q = \frac{\mu \cdot U \cdot I}{v_z} \quad \left[\frac{J}{mm}\right] \tag{3}$$

$$Q_c = Q \cdot L_z \quad [J] \tag{4}$$

The total heat delivered to the weldment (Q_c) was calculated based on the determined weldment length. The obtained and calculated values of the welding process parameters are shown in Tables No. 4 and 5.

Table 4 Obtained and calculated parameters of the welding process; weldment A variant

Specimen No.	*Q [J/mm]*	*t_z [s]*	*L_z [mm]*	*Q_c [J]*
1A	76.8	12.5	187.5	14400.0
2A	88.8	10.5	158.4	14065.9
3A	100.3	11.8	178.3	17860.0

Table 5 Obtained and calculated parameters of the welding process; weldment B variant

Specimen No.	*Q [J/mm]*	*t_z [s]*	*L_z [mm]*	*Q_c [J]*
1B	76.8	12.2	184.1	14142.0
2B	88.8	12.4	186.0	16516.8
3B	100.3	13.1	196.7	19722.0

The obtained data was then used to analyse the course of angular deformations (Figures 4 and 5). The resulting angular deformations developed depending on the weldments geometry, welding parameters as well as mechanical properties of the materials being welded. Positioning of the weldment, burner guiding, direction of the filler material on the flange or the web of the materials being welded also significantly affect the weldments deformation. The heat source cannot always be ideally directed so that the weld bead is made exactly along the axis between two materials being joined. Deformation extent is also influenced by the inner structure and chemical composition of the welded materials. The stresses introduced into the weld joint are not manifested by equally large deformations in individual weldments.

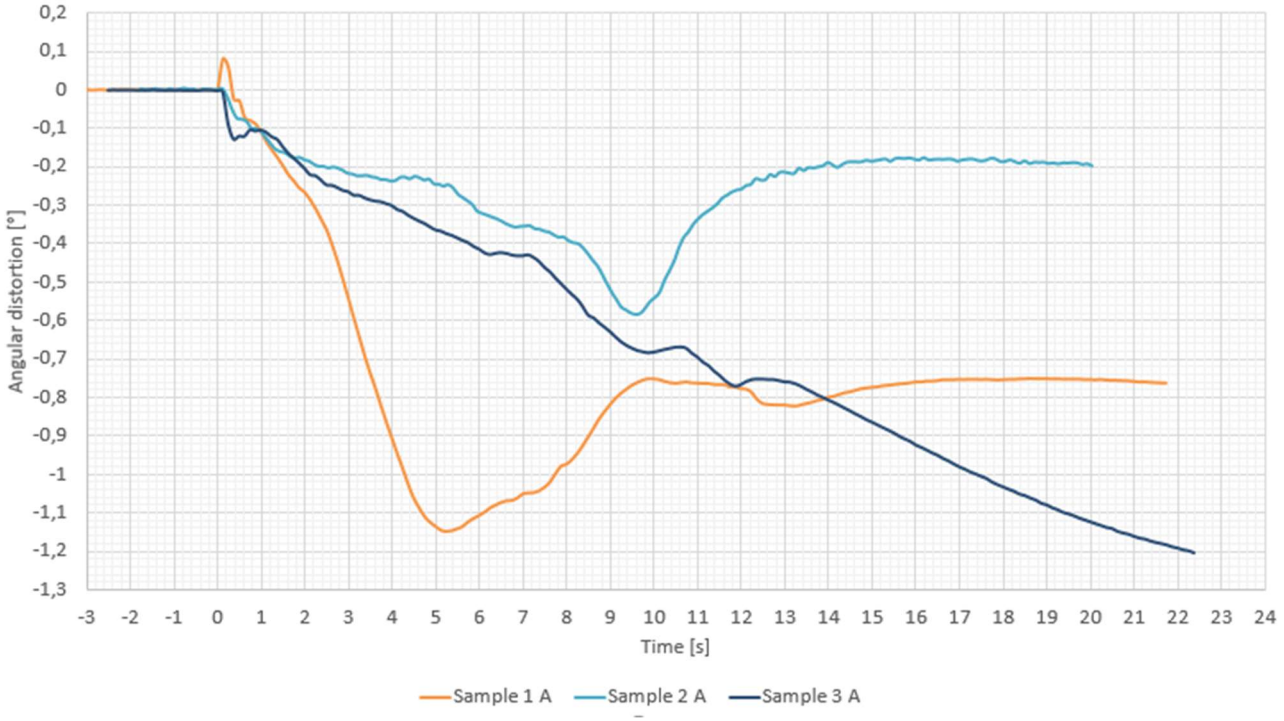

Fig. 4 Time curve of angular deformations, variant A

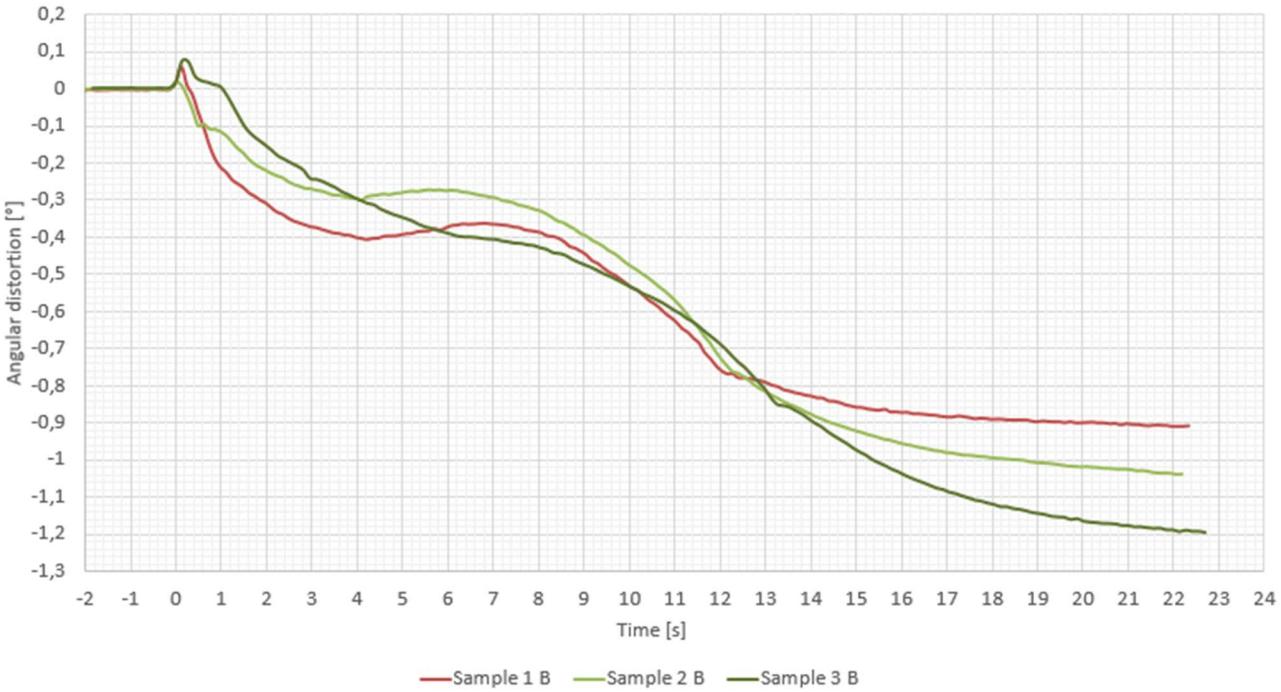

Fig. 5 Time curve of angular deformations, variant B

The data analysis suggests that larger angular deformations and shape deviations occur when larger total heat is supplied to the weldment. The curve of angular deformations varies depending on the welding geometry of variants A and B. The total heat (Q_c) supplied into the weldment throughout the entire length of the weld joint affects the size of the generated stress, which, upon release, is manifested as deformations.

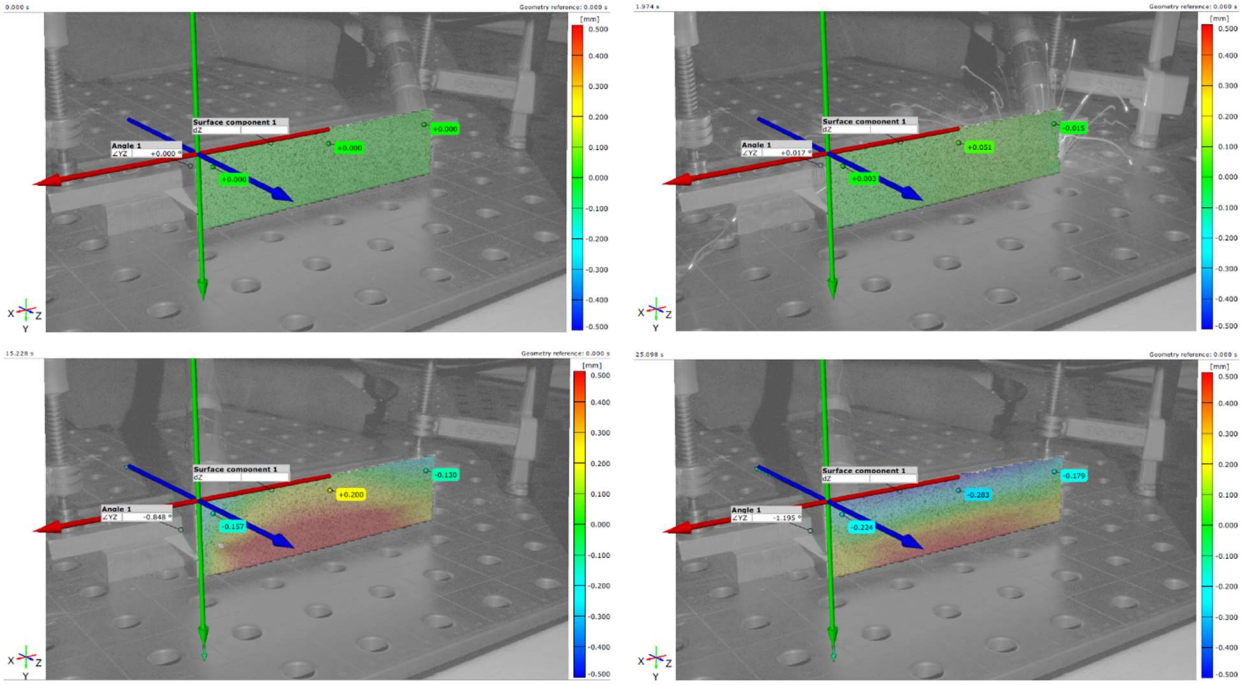

Fig. 6 Colour map of deviations along the axis direction and angular deformation of specimen No. 3B; a) reference scan (t: 0.00 s); b) beginning of welding (t: 1.97 s); c) end of welding (t: 15.23 s); d) cooling the weldment (t: 25.10 s)

The welding current of 90 A of specimen No. 2 A created lower overall heat delivered to the weldment which resulted in lower rate of deformations at a given weldment length than in the case of welding the specimen No. 1 A.

The data records from scanning can be used to build colour maps of shapes deviations in the specified direction (Figure 6). After determining a reference record image, the analysis of colour deviation map can be used to track the displacement values of individual weldment points during the welding process.

4. Conclusion

The welding process executed by using the portal equipment and the Fronius TPS600i welding machine provides a complete control over the welding process as well as precise observance of the technological parameters throughout the welding time (specific heat input). Course and development of the weldments deformations depend on the welding method used, heat input, total heat supplied, weldment geometry and the type of welded material. The resulting records allow for tracking the real-time course of weldments deformation at a frequency of 15 Hz, which is sufficient for welding processes. When scanning, it is however necessary to prevent the incident light of the electric arc into the scanning lenses, which can be achieved by welding geometry and scanning the weldment from the reverse side. The process of non-contact measurement of free-form surfaces thus finds application also in the technology field of welding.

5. Acknowledgements

This work was supported by the project: ITMS 26210120017 “Centre for research and development in the field of the electron-beam and progressive arc technologies of welding, cladding and surface-finishing”.

The authors express their thanks to the MCAE Systems, s.r.o. Company for providing the software equipment and valuable advice in addressing the field of scanning.

6. References

[1] Foster, S. & Halbstein, D., 2014. *Integrating 3D Modeling, Photogrammetry and Design.* s.l.: Springer London Heidelberf New York Dordrecht, ISBN 978-1-4471-6329-9.

[2] Hartley, R. & Zisserman, A., 2004. *Multiple View Geometry in Computer Vision.* Australian National University, Canberra, Australia - University of Oxford, UK, ISBN 978-0-511-18618-9: Cambridge University Press 2000, 2003.

[3] GOM Testing, Digital Image Correlation and Strain Computation Basics, Technical Documentation of V8 SR1, GOM mbH, 2016, EN 21-01-2016

[4] Feng, Z., 2005. *Processes and mechanisms of welding residual stress and distortion.* Cambridge: Woodhead Publishing Limited, ISBN-13:978-1-84569-093-9.

[5] Luhmann, T., Robson, S., Kyle, S. & Harley, I., 2006. *Close Range Photogrammetry. Principles, Methods and Applications.* Scotland, UK: ISBN 1-870325-50-8.

[6] Aluminium Alloy Datasheet 5083. 2013. Available at: <http://www.atlassteels.com.au/documents/Atlas_Aluminium_datasheet_5083_rev_Oct_2013.pdf>

[7] BUNAZIV, I., AKSELSEN, O. M., SALMINEN, A. , UNT, A. 2016. Fiber laser-MIG hybrid welding of 5 mm 5083 aluminum alloy. Available at: <http://www.sciencedirect.com/science/article/pii/S0924013616300528>

[8] JESUS, J.S., GRUPPELAAR, M., COSTA, J.M., LOUREIRO, A., FERREIRA, J.A.M. 2016. Effect of geometrical parameters on Friction Stir Welding of AA 5083-H111 T-joints. Available at: <http://ac.els-cdn.com/S2452321616000342/1-s2.0-S2452321616000342-main.pdf?_tid=d0855b5e-b598-11e6-8aa1-00000aacb362&acdnat=1480358042_5a8cbd3300c2a712c75beb63c99a0f4b>

[9] PARK, S.-H, KIM, J.-S., HAN, M.-S., KIM S.-J. 2009. Corrosion and optimum corrosion protection potential of friction stir welded 5083-O Al alloy for leisure ship. Available at: <http://www.sciencedirect.com/science/article/pii/S1003632608603738>
[10] ASM INTERNATIONAL HANDBOOK COMMITTEE. 1990. Metal Handbook. 90-115, USA, ISBN 0-87170-378-5 (V. 2)
[11] 5083 -'0'-H111 Sheet and Plate, Aalco Metals Limited [cit. 2016-11-23]. Available at: <http://www.aalco.co.uk/datasheets/Aluminium-Alloy_5083-0~H111_149.ashx>
[12] 5083 Aluminum Plate [cit. 2016-11-23]. Available at: < http://www.twmetals.com/5083-aluminum-plate.html>
[13] SIDHOM, N., MOUSSA, B. N., JANEB, S., BRAHAM, Ch., SIDHOM, H. 2014. Potential fatigue strength improvement of AA 5083-H111 notched parts by wire brush hammering: Experimental analysis and numerical simulation. Available at: <http://www.sciencedirect.com/science/article/pii/S0261306914006074>